Hydrogen-Induced Amorphization of Nd_3Ga and Sm_3Ga Compounds with DO_<19> Structure

Hydrogen-Induced Amorphization of Nd_3Ga and Sm_3Ga Compounds with DO_{19} Structure*

XingGuo Li**, Kiyoshi Aoki and Tsuyoshi Masumoto

Institute for Materials Research

(Received October 20, 1988)

Synopsis

Structural changes of c-R_3Ga (R = Nd, Sm) compounds having the DO_{19} structure during the hydrogen absorption process were investigated by x-ray diffraction, electron microscopy, and the thermal analysis. By hydrogenation of c-Nd_3Ga and c-Sm_3Ga compounds, an amorphous single phase a-$Nd_3GaH_{6.2}$ and a-$Sm_3GaH_{5.9}$ was formed between 300 K and 400 K, respectively. However, hydrogenation of the compounds gave rise to the transformation from the DO_{19} phase to c-Nd_3GaH_x and c-Sm_3GaH_x having the fcc structure above 450 K. Crystallization of the hydrogen-induced amorphous alloys was studied by differential scanning calorimetry from which the crystallization temperature, the enthalpy change, and the activation energy of crystallization were determined.

I. Introduction

Hydrogen-induced amorphization (HIA), that is, the transformation from the crystalline to the amorphous state by hydrogen absorption, has received much attention as a new process for the preparation of amorphous alloys. Although it has been reported that HIA occurs in many intermetallic compounds having the $L1_2$ (1-3), C15 (4-8), C23 (9), and DO_{19} (10) structure, its mechanism is still uncertain. In order to make clear the mechanism of HIA, it is essential to know the alloy types and the conditions under which the compounds become amorphous. In an attempt to answer this, structural changes of the R_3Ga

compounds, which are suggested to be the $L1_2$ alloys, during the hydrogen absorption process were investigated. In this paper the formation of the amorphous phases and crystallization of the resultant amorphous alloys are described.

II. Experimental

The Nd_3Ga and Sm_3Ga compounds were prepared by arc melting using high purity metals [Nd,Sm(99.9%) and Ga(99.99%)] in a gettered argon gas atmosphere. The ingots were homogenized at 923 K for 605 ks in an evacuated quartz tube. The ingots were cut into small blocks for hydrogen absorption. After the activation treatment at 300 K for 3.6 ks in a vacuum, the samples were reacted with high purity hydrogen (7N) of 5 MPa between 300 K and 573 K for 86.4 ks. The amount of hydrogen absorbed was determined by measuring the change of H_2 pressure in a constant volume reactor. Structures of the samples before and after hydrogenation were identified with x-ray diffraction (XRD) using the monochrometed CuKα radiation. Some samples were further examined by transmission electron microscopy (TEM). The crystallization behavior of the hydrogen-induced amorphous alloys were examined by differential scanning calorimetry (DSC) at various heating rates in an argon atmosphere.

III. Results and discussion

Figure 1 (a) shows powder XRD patterns of the Nd_3Ga compound hydrogenated at various temperatures along with the original one. It has been proposed that the Nd_3Ga compound has an $L1_2$ structure (10). However, the XRD pattern of the present homogenized sample could not be indexed based on the $L1_2$ structure. Instead, the pattern was satisfactorily indexed on the basis of the DO_{19} structure. The lattice parameter of the sample having the DO_{19} structure is a = 0.728 nm and c=0.568 nm. In the XRD patterns of the samples hydrogenated at 300 K and 373 K, however, the sharp Bragg peaks completely disappear and only a broad maximum is observed. At a higher hydrogenation temperature above 473 K, new Bragg peaks corresponding to the fcc structure appear.

Figure 2 shows a bright field image (a) and the corresponding diffraction pattern (b) of the Nd_3Ga sample fully hydrogenated at 300K. The lack of the contrast in the bright field image and the
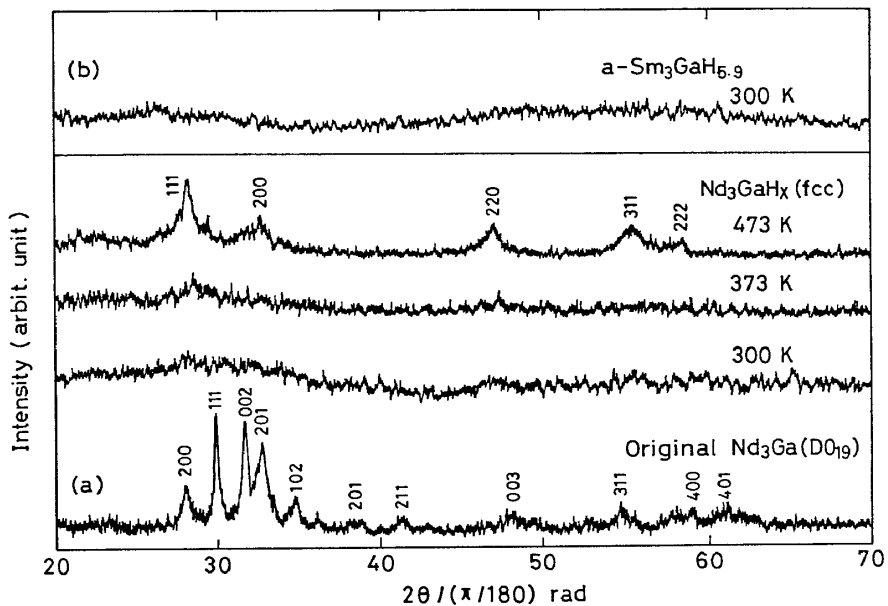
Figure 1   The   powder XRD patterns of the Nd$_3$Ga
and Sm$_3$Ga compounds hydrogenated at various temperatures.

diffuse halo on the diffraction
pattern indicate that the
hydrogenated sample has an
amorphous structure similar to that
observed in normal amorphous alloys
prepared by the conventional
technique. The amount of hydrogen
absorbed in this alloy   is 1.55
(H/M) (hydrogen atoms per one
metal), so that the amorphous alloy
can be written as a-Nd$_3$GaH$_{6.2}$.

Figure 2   A transmission electron
micrograph (a) and diffraction
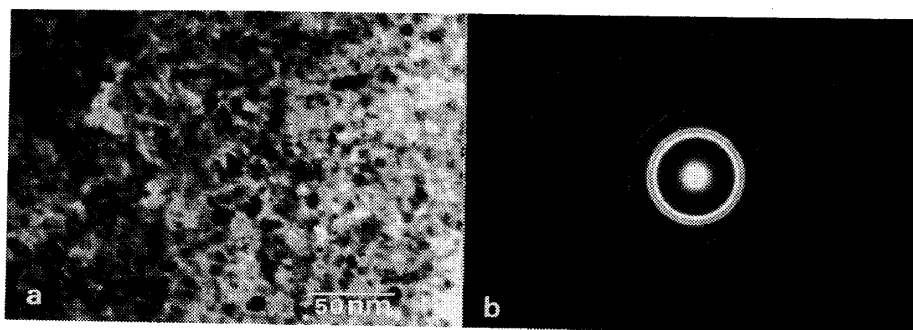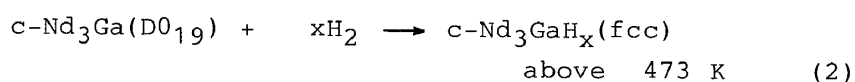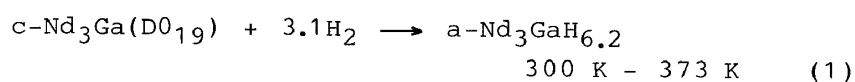pattern (b) of a-Nd$_3$GaH$_{6.2}$
hydrogenated at 300 K.
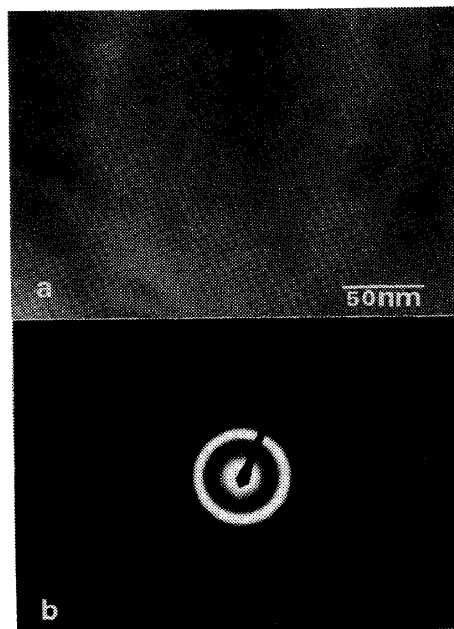
Figure 3　　A bright field image (a) and the corresponding
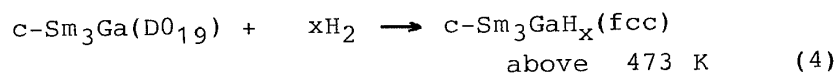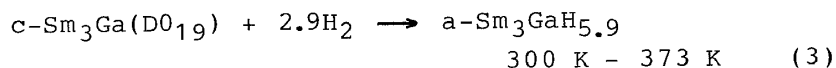diffraction pattern (b) of $a\text{-}Nd_3GaH_{6.2}$ hydrogenated at 473 K.

Figure 3 shows a bright field image of the sample hydrogenated at
473 K (a) and the corresponding diffraction pattern (b). The bright
field image shows homogeneous precipitates, and the diffraction
pattern can be indexed based on the single phase of the fcc structure
with a lattice parameter of a = 0.533 nm. The lattice parameter of the
present alloy is nearly same as that of NdH_2 having the fcc structure
(a=0.547 nm)(11). However, the product is not NdH_2, because the
formation of NdH_2 alone is irrational from the material balance. We
conclude that the product is $c\text{-}Nd_3GaH_x$ having the fcc structure of　a
= 0.533 nm. Therefore, the reaction product of $c\text{-}Nd_3Ga$ with hydrogen
gas changes with increasing temperature as follows:

$$c\text{-}Nd_3Ga(DO_{19}) \ + \ 3.1H_2 \ \longrightarrow \ a\text{-}Nd_3GaH_{6.2}$$

300 K - 373 K 　　(1)

$$c\text{-}Nd_3Ga(DO_{19}) \ + \ xH_2 \ \longrightarrow \ c\text{-}Nd_3GaH_x(fcc)$$

above　473 K 　　(2)

Hydrogenation of $c\text{-}Nd_3Ga$ gives rise to the transformation from
the DO_{19} to the fcc structure above 473 K. This transformation is not
so strange and is sometimes observed(12). In the present alloy the fcc
structure is stablized by hydrogen.

Next we discuss structural changes of $c\text{-}Sm_3Ga$ during the hydrogen
absorption process. The present work confirms that the crystal
structure of $c\text{-}Sm_3Ga$ is DO_{19}, although it has been proposed that c-
Sm_3Ga has the $L1_2$ structure(10). The lattice parameter of $c\text{-}Sm_3Ga$ is
a = 0.714 nm and c = 0.557 nm. As an example, the XRD pattern of the
Sm_3Ga hydrogenated at 300 K is shown in Fig. 1(b). In the 　XRD
patterns of the samples hydrogenated below 373 K, the sharp Bragg
peaks completely disappear and only a broad maximum is observed.

Further, both the bright field image and the electron diffraction pattern confirm the amorphous nature of the alloys. The reaction product of c-Sm$_3$Ga with hydrogen is as follows:

$$c\text{-Sm}_3\text{Ga}(DO_{19}) + 2.9H_2 \longrightarrow a\text{-Sm}_3\text{GaH}_{5.9}$$
$$300 \text{ K} - 373 \text{ K} \qquad (3)$$

$$c\text{-Sm}_3\text{Ga}(DO_{19}) + xH_2 \longrightarrow c\text{-Sm}_3\text{GaH}_x(\text{fcc})$$
$$\text{above} \quad 473 \text{ K} \qquad (4)$$

The lattice parameter of c-Sm$_3$GaH$_x$ (fcc) is 0.540 nm. HIA in c-Sm$_3$Ga occurs under the same situation of that in c-Nd$_3$Ga. Since HIA occurs when the formation of the most stable phases in the metal-hydrogen system is suppressed kinetically(3-7), it is important to know the reaction products at elevated temperatures. HIA of the Laves phases RM$_2$(C15) and the Ce$_3$Al(DO$_{19}$) occurs at the temperatures where the decomposition into RH$_2$ and M, and CeH$_2$ and CeAl$_2$ is suppressed, respectively. On the other hand, HIA of c-Zr$_3$In(fcc) occurs at the temperatures where the formation of c-Zr$_3$InH$_x$(fcc) is suppressed (3). That is, the HIA behavior of R$_3$Ga is similar to that of c-Zr$_3$In. The present authors have proposed that the ocurrence of HIA in the Laves phase RM$_2$ compounds is closely related to the formation of the elemental hydride at elevated temperatures. In the present compounds, however, the decomposition into RH$_2$ and Ga is not observed. Therefore, HIA in R$_3$Ga compounds may be controlled by the another mechanism. The clarification of the HIA mechanism in these compounds is the subject for a future study.
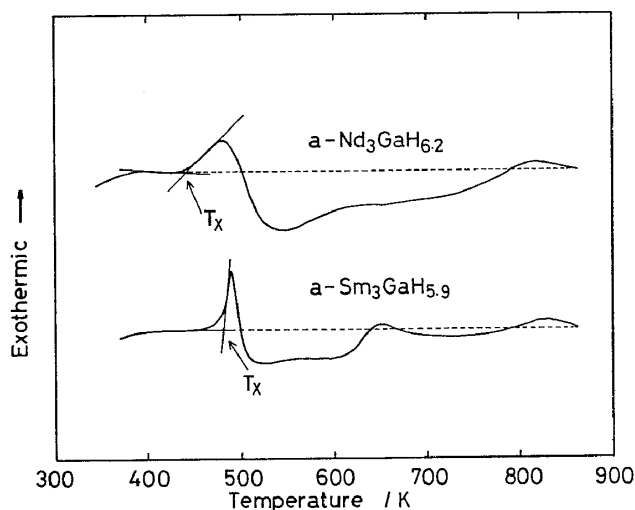

Figure 4 The DSC curves of hydrogen-induced amorphous a-Nd$_3$GaH$_{6.2}$ and a-Sm$_3$GaH$_{5.9}$.

Figure 4 shows DSC traces of a-$Nd_3GaH_{6.2}$ and a-$Sm_3GaH_{5.9}$ prepared by hydrogenation at 300 K. An exothermic peak along with a broad endothermic peak are observed. To clarity the nature of the peaks, structures of the samples heated to several stages were examined by XRD and TEM. Since the electron diffraction pattern of a-$Nd_3GaH_{6.2}$ heated to 433 K shows only a halo, it is concluded that the amorphous structure is retained at this temperature. The bright field image and the corresponding electron diffraction pattern of the sample heated to 543 K are same almost as those in Fig. 2. Therefore, we conclude that the exothermic peak is due to crystallization of the hydrogen-induced amorphous alloy. In addition, no endothermic peak resulting from hydrogen desorption is observed below the exothermic peak in contrast to a-RM_2H_x(4-7). This suggests that hydrogen atoms in a-R_3GaH_x are more tightly trapped than those in a-RM_2H_x and that the hydrogen content does not change. Therefore, crystallization of a-$Nd_3GaH_{6.2}$ is expressed as follows

$$a\text{-}Nd_3GaH_{6.2} \longrightarrow c\text{-}Nd_3GaH_{6.2} \tag{5}$$
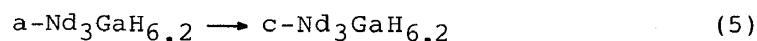
Similarly, crystallization of a-$Sm_3GaH_{5.9}$ is expressed as follow:
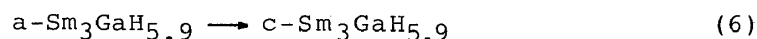
$$a\text{-}Sm_3GaH_{5.9} \longrightarrow c\text{-}Sm_3GaH_{5.9} \tag{6}$$

The crystallization temperature T_x, the enthalpy change ΔH_c of crystallization, and the activation energy E_a for crystallization of the hydrogen induced a-$Nd_3GaH_{6.2}$, a-$Sm_3GaH_{5.9}$, and related amorphous alloys are listed in Table 1. In the present work, T_x was defined as the temperature corresponding to the intersection of the extrapolated base line and the steepest tangent to the first exothermic peak observed in DSC at a heating rate of 40 K/min, ΔH_c was calculated from the exothermic peak area, and E_a was determined using the Kissinger method. A plot of $\ln(\phi/T_p^2)$ vs $1/T_p$ gives a straight line of the gradient $-E_a/R$ as seen in Fig.5, where T_p is the peak temperature and ϕ is a heating rate. T_x of a-$Nd_3GaH_{6.2}$ and a-$Sm_3GaH_{5.9}$ is 438 K and 468 K, respectively, and T_x of each alloy is in agreement with the highest temperature of the formation of a-R_3GaH_x alloys during the hydrogen absorption process. ΔH_c of a-R_3GaH_x alloys is about -1 kJ/mol, which is about one third of other hydrogen induced amorphous alloys(13-14). E_a of a-R_3GaH_x alloys is about 85 kJ/mol, which is about half of other amorphous alloys. Thus, T_x, H_c and E_a, especially the later two in a-R_3GaH_x alloys are considerably lower in comparison with those of a-$Nd_2AlH_{5.4}$ and

Table 1   Thecrystallization temperature T_x, the enthalpy change ΔH_c of crystallization, and the activation energy E_a of crystallization of hydrogen induced amorphous alloys.

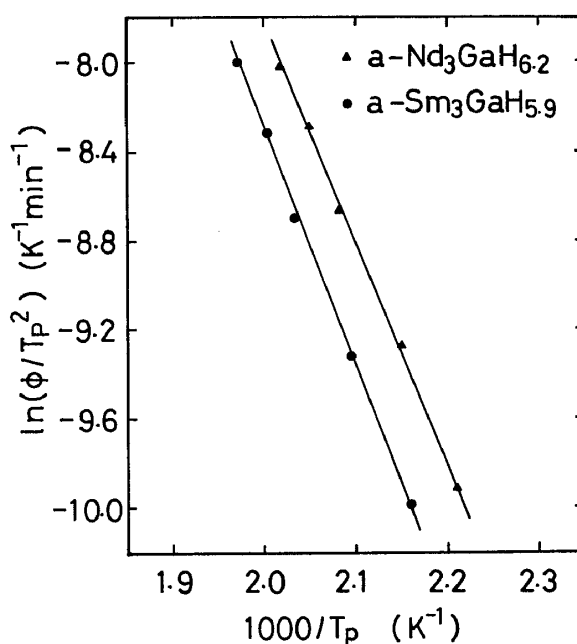| Alloys	ΔH_c(kJ/mol)	E_a(kJ/mol)	T_x(K)
a-Nd$_3$GaH$_{6.2}$	-1.0	84	438
a-Sm$_3$GaH$_{5.9}$	-1.1	86	469
a-Nd$_2$AlH$_{5.4}$(13)	-3.1	158	480
a-RM$_2$H$_x$(14)	-3.3	151	647

Figure 5   Kissinger plots of a-Nd$_3$GaH$_{6.2}$ and a-Sm$_3$GaH$_{5.9}$ obtained from continuous heating experiments.

a-RM$_2$H$_x$. These imply that the a-R$_3$GaH$_x$ (R = Nd, Sm) alloys are thermally more unstable. The a-R$_3$GaH$_x$ alloys crystallize polymorphously to c-R$_3$GaH$_x$, while the other amorphous alloys a-Nd$_2$AlH$_x$ and the a-RM$_2$H$_x$ decompose into NdH$_2$ + NdAl$_2$ and RH$_2$ + M, respectively. The lower ΔH_c and E_a values may be due to the fact that a-R$_3$GaH$_x$ crystallize polymorphously to the closed packed c-R$_3$GaH$_x$ without no long range diffusion of metal atoms.

IV. Summary and conclusions

By hydrogenation of the c-Nd$_3$Ga and c-Sm$_3$Ga compounds having the DO$_{19}$ structure, the amorphous a-Nd$_3$GaH$_{6.2}$ and a-Sm$_3$GaH$_{5.9}$ alloys could be prepared below 373 K. However, the compounds became c-R$_3$GaH$_x$ with the fcc structure above 470 K. Crystallization of the hydrogen-induced amorphous alloy was investigated by scanning differential calorimeter (DSC) from which the crystallization temperature T_x, the enthalpy change ΔH_c of crystallization and the activation energy E_a for amorphization were determined. Both ΔH_c and E_a of the present amorphous alloys are considerably lower than those of other hydrogen-induced amorphous alloys.

Acknowledgements

References

(1) X.L.Yeh,K.Samwer and W.L.Johnson, Appl. Phys. Lett., **42**(1983)242.

(2) M.Komatsu, H.Fujita and Y.Ishiii, Collected Abstr. Annual Meeting Japan Inst. Metals,(1984)209.

(3) K.Aoki, X.G.Li, K.Chattopadhyay and T.Masumoto, Scripta Metall., **22**(1988)991.

(4) K.Aoki, K.Shirakawa and Masumoto, Sci. Rep. RITU, **A-32**(1985)239.

(5) K.Aoki,T.Yamamoto,T.Masumoto, Scripta Metall., **21**(1987)27.

(6) K.Aoki,M.Nagano,A.Yanagitani and T.Masumoto, J. Appl. Phys., **62** (1987)3314.

(7) K.Aoki, A.Yanagiani, X.G.Li and T.Masumoto, Mat. Sci. and Eng., **97**(1988)35.

(8) K.Aoki, X.G.Li,T.Masumoto,MRS,International Meeting on Advanced Materials,Tokyo, Japan May 30-June 3 (1988).

(9) X.G.Li, K.Aoki and T.Masumoto, Proceedings of JIMIS-5:Non-Equilibrium Solid Phases of Metals and Alloys. Supplement to Trans.JIM, **29**(1988)105.

(10) A.Iandelli, "The Physical Chemistry of Metallic Solution and Intermetallic Compounds", Natl. Phys. Lab., Gt. Brit., Symp.

194

no.9, Vol. I, 3F, (1959)11.

(11) K.A.Gschneidner, Jr, L.R.Eyring, "Handbook on the Physics and Chemistry of Rare Earths", Vol 3, North-Holland Publishing Company (1979)p307.

(12) J.H.N. van Vucht, Z.Metallk., 48(1957)253, Philips Res. Rept. 16(1961)1.

(13) X.G.Li, K.Aoki, T.Masumoto, unpublished work.

(14) T.Aihara, K.Aoki, T.Masumoto, unpublished work.